

# AUTOMATIC CALIBRATION OF A MOTION CAPTURE SYSTEM BASED ON INERTIAL SENSORS FOR TELE-MANIPULATION

Jörg Hoffmann

*Institut für Informatik II, University of Bonn, Germany*  
*hoffmann@cs.uni-bonn.de*

Bernd Brüggemann

*Fraunhofer Institute for Communication, Information Processing and Ergonomics (FKIE), Wachtberg, Germany*  
*bernd.brueggemann@fkie.fraunhofer.de*

Björn Krüger

*Institut für Informatik II, University of Bonn, Germany*  
*kruegerb@cs.uni-bonn.de*

**Keywords:** Telerobotics and Teleoperation, Motion Capturing, Automatic Calibration, Inertial Sensors

**Abstract:** We introduce an intuitive way of controlling a manipulator. This control should fulfill several constraints like low room consuming and operable in a short time. With this constraints in mind we chose an inertial sensor based motion capturing system. Such systems have to be adapted to the user. We present a method to adapt the system by a fast calibration while it is been used. The calibration does not require specified given motions. The soundness of the system is shown in synthetic and real experiments.

## 1 INTRODUCTION

Interactive manipulation of their environment is an essential task for robots. To provide a good tool for manipulation in most cases robots are equipped with a robot arm. Controlling such a manipulator is a challenging task, especially if it should be remotely controlled. The operator usually has an impression about the environment by video only. Based on this few information he has to perform complex motions with a manipulator. Controlling each joint separately demands long previous training and high concentration. The operator has to plan a sequence of motions for each joint in advance. The difficulty of these operations is raised by the fact that it may be necessary to re-adjust the joints during the motions.

As part of danger defence and disaster response exploring a potential dangerous area without exposing persons becomes more and more important. On one hand, threats by terrorist groups can cause great damage with relatively small effort. On the other hand, disasters in industrial areas may release dangerous and not easily detectable chemicals (TICs). If such an emergency occurs, information about what has happened and how the situation is developing is crucial for an effective response. Here robots can help to acquire desired information without exposing personnel to unknown risks. Such robots can be equipped with several sensors to identify different threats. But often

it is just as important to manipulate the environment. This may occur e.g. if a suitcase has to be opened, or a sample has to be taken for analysis.

Nowadays most robots, which are meant to be used within a disaster area are at least partly remote controlled. So the operator has no direct line of sight to the robot and the area the robot is working in. Being reliant on only few sensors (like a camera) complex manipulations have to be executed. Often such tasks are time critical and far away from any available infrastructure. Therefore the needed control method for the robot arm has to fulfill several constraints: Intuitively usable, can be employed quickly, space saving and easy to transport, and pose only small restrictions to the mobility of the user

In this paper we present a method to steer the manipulator directly by the operator's movements without the need of an exoskeleton. We use five inertial sensors to capture the motions of the operator. The most important part in our system is the auto-calibration which makes an exact sensor placement unnecessary. In fact we only need to know roughly where the sensors are positioned.

The remainder of the paper is organized as follows: In section 2 related works are presented and different ways of remotely controlled manipulators are shown. In section 3 the problem and its constraints are described while section 4 shows the preprocessing of the sensor signals. The automatic calibration

for our inertial sensor based motion capturing system is presented in section 5, followed by the robot arm control mechanism in section 6. Section 7 presents results of the calibration as well as its effect on the direct manipulation controls. The paper closes with our conclusions.

## 2 RELATED WORK

### 2.1 Robot Arm Control

Industrial robots are the prime example of the market's demand of manipulators. But also in mobile robotics the control of manipulators is essential. Here, in contrast to the industrial robots, the movement is not predefined and has to be adapted to the situation and the task. So, in the course of time several different methods for controlling a manipulator were developed. Roughly those methods can be divided into remotely controlled and autonomous movements.

Remotely controlled drives have the advantages to fall back on the decision of the operator. Although there is no need of autonomous decisions the system has to provide the operator with full control and information needed for the motion task. Within the remotely controlled manipulators, methods can be distinguished by their input devices, e.g. joysticks (some mentioned in (Laycock and Day, 2003)). From standard joysticks to those with force feedback, the boundaries to master-slave control mechanisms are fluid.

The idea to couple a control mechanism directly to the manipulator is rather old (e.g. (Goertz, 1954)). Such master-slave approaches have some advantages like being very accurate and the operator is always aware of the motions the manipulator will perform. Additionally, master-slave controls are able to provide the operator with haptic feedback. So there can be more resistance within the master device if the manipulator will be near to an obstacle or it is possible to feel the structure of a surface (e.g. (Tachi et al., 1990; Yokokohji and Yoshikawa, 1992)).

In-between master-slave devices and joysticks, there are exoskeletons. Such devices are worn by the operator. Exoskeletons are available for just a limb (e.g. an arm) or as whole body device (Bergamasco et al., 1994). Its advantages are a very precise reconstruction of the human motion and, compared to the master-slave approach, less space is needed. But due to the stiff construction, those exoskeletons prevent the operator from performing movements in a natural way.

Motion capturing is another approach to control a manipulator by reconstructing human movements. (e.g. (Miller et al., 2004; Pollard et al., 2002)). Approaches range from camera based motion capturing (with active or passive markers) to motion capturing with inertial sensors.

### 2.2 Motion Capturing with Inertial Sensors

Many techniques for capturing human motions have been developed in the last decades. Most of these techniques suffer from several disadvantages: they are not portable, need complex calibrations, or have disturbing exoskeletons. A good overview over the most important techniques is given in (Welch and Foxlin, 2002).

In the last years inertial sensor systems have become more popular for many applications. They are used for action recognition in games (Slyper and Hodgins, 2008), and for detection of typical or similar patterns in medical applications (Sabatini et al., 2005; Chang, 2006). A lot of work has been done on partial motion capturing, where only special parts of the body, as upper limbs for example, are considered. In this area applications like home rehabilitation systems (Zhou et al., 2006; Zhou and Hu, 2007; Tao et al., 2007) or robot controllers (Miller et al., 2004) have been developed. For tracking applications several systems based on fusion of inertial sensors and a variety of other systems have been introduced (Foxlin, 2005). For full body motion capturing a portable system based on inertial sensors combined with an acoustic system was designed (Vlasic et al., 2007). Since Nintendo introduced the Wiimote in 2006 a lot of applications were developed (Schou and Gardner, 2007; Lee, 2008; Shiratori and Hodgins, 2008), while low cost sensors are available for mass market applications.

All these applications have to face similar technical difficulties. The data of inertial sensors are noisy and may contain a drifting. This problem is tackled using some basic techniques in all applications. Kalman filters are widely used for an optimal estimation based on data of multiple sensors (Vlasic et al., 2007; Zhou and Hu, 2007; Tao et al., 2007; Shiratori and Hodgins, 2008), especially when different types of sensors are combined. A Monte Carlo optimization can be used as basis for the estimation of positions and orientations (Zhou et al., 2006). For recognition of typical patterns in acceleration data classical signal processing techniques, like phase detection (Sabatini et al., 2005) or frequency analysis by Haar wavelet transformations (Slyper and Hod-

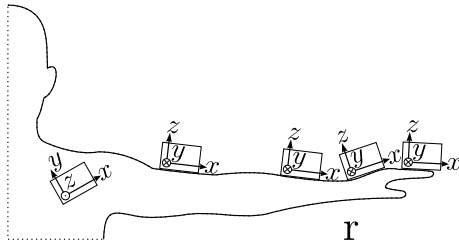


Figure 1: Positioning of the five inertial sensors on the right arm. Each joint is assigned to one sensor. The sensor on the shoulder is used as fix point.

gins, 2008) have been employed. To estimate the direction of gravity several heuristics have been developed (Miller et al., 2004; Foxlin, 2005).

### 3 PROBLEM DESCRIPTION

To directly control the robot manipulator, the movement of the whole human arm has to be reconstructed. Therefore, we used four inertial sensors. One for each part of the arm: Upper arm, lower arm, hand, and fingers. A fifth sensor is needed to be positioned on the shoulder as a fix point (see Figure 1). The sensors provide their orientation but no information about their position in space. If the setup of the human arm and each sensor positioning on that arm is known, then it is possible to compute the arm configuration:

Let  $G_i$  be the missing position for the  $i$ -th joint,  $q_i$  the orientation measured by sensor  $i$  and  $s_i$  the length of the segment  $i$  (from joint  $i$  to  $i + 1$ ).  $R_{q_i}(v)$  is the rotation of vector  $v$  around  $q_i$ . Then the desired positions of each joint are:

$$G_0 = [0, 0, 0]^T \quad (1)$$

$$G_i = G_{i-1} + R_{q_i}([s_i, 0, 0]^T) \quad (2)$$

Those equations needs the sensors to be oriented in direction of the bone it is connected to. Unfortunately the positioning of the sensors in reality is not as accurate as it is needed. So each sensor has a bias to the desired positioning. Figure 2 shows such a situation. Assuming the positioning is accurate, the orientations of the sensors imply a bended arm. When taken the faulty positioning  $\alpha$  and  $\beta$  into account it can be recognized that the original arm configuration corresponds to a stretched arm. If the sensors are placed carefully on the human arm, the result will be alright but not very precise. But for a trustworthy and accurate result it is important to know the difference between the bone orientation and its corresponding sensor.

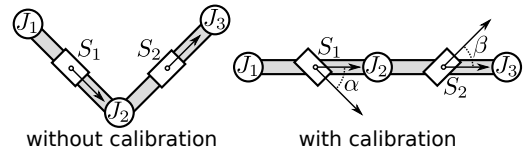


Figure 2: Imprecise positioning of sensors will cause false reconstruction of movements. Assuming the sensors are placed carefully the orientation implies a bended arm (left). When knowing that the sensors are placed faulty by an angle  $\alpha$  and  $\beta$  the arm has to be reconstructed as stretched (right).

When the system is calibrated, the reconstructed motions of the operator can be used to control the manipulator. As the used manipulator (and many robot arms currently available) has not the same morphologies as the human arm, it is not possible to map the reconstructed joint angles directly to the robot. So another mapping has to be found. We used a simple mapping by directly using the position and orientation of the operator's fingers. These informations are easy to compute with the calibrated arm model. As the finger's position is related to the shoulder, it can be used to provide a target for the manipulator's tool center point (TCP). This means that there will be no direct correlation between the pose of the human arm and the manipulator but a correlation between the position of the fingers and the TCP.

## 4 SIGNAL PREPROCESSING

We use two different types of sensor data provided by the inertial sensor system. First, we get orientation data which are used to perform forward kinematics on our arm model. Second, we obtain acceleration data which are used for the calibration. While the orientation data is reliable over long time periods the acceleration data is more noisy and is afflicted by drifting. In this section we show how we proceed with these artifacts in our sensor data.

### 4.1 Removing Noise

We have to remove noise on both sensor signals: The orientation data and the acceleration data. Both data types have a high frequency noise. To reduce this noise, we used a standard binomial low pass filter. As the velocity signal is a function in the position space, a filter with a window  $w = 20$  data points is chosen. Since the orientations are represented by quaternions, we employ a smoothing filter to the orientation data like it is described by (Lee and Shin, 2002) in order to achieve reliable data.

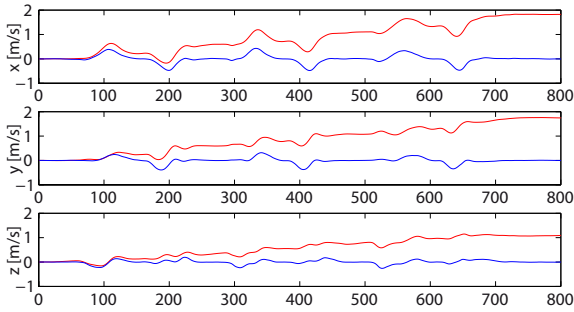


Figure 3: Velocity data for the three axis. Without zero velocity updates the data show a clear drift (red), with zero velocity updates the drift is visibly reduced (blue).

## 4.2 Removing Drifting

The acceleration measurements include the gravitation. These so-called local accelerations have to be converted to global acceleration, i.e. accelerations without gravitation. When using the sensor orientation to remove acceleration caused by gravity, small errors in the orientation accumulate to large drifts in the rotational acceleration.

We can efficiently remove drifting by applying zero velocity updates (ZUPT) introduced by (Grejner-Brzezinska et al., 2001). Regardless whether we know the exact positions and orientations of our sensors: If the orientations do not change neither will the positions. We computed the velocity of each joint of our arm model. If these velocities are slower than a threshold (we use  $0.05 \frac{\text{m}}{\text{s}}$ ) we presume that the arm is not moving, i.e. its accelerations are zero. The measured non zero accelerations at these zero velocity points describe how the data have drifted. We use these information to correct the acceleration between two zero velocity points by changing the accelerations linearly. Some results of this method are given in Figure 3. Without zero velocity updates the data show a clear drift away from the zero line, with zero velocity updates the drift is visibly reduced. It shows that the sensor drifting can be removed clearly. Note that this technique is an offline strategy. However, this is no drawback, since we need the acceleration data only for the calibration of the sensors. For reconstruction we only use the orientation data, which do not have any drifting at all.

## 5 SENSOR CALIBRATION

The goal of our calibration is to detect the sensors' positions and orientations on the operator's arm automatically. Figure 2 shows the importance of this

step, since a wrong bias may lead to faulty reconstructions of the arm motions. During our calibration step we use a model of the human arm. This model consists of four by spherical joints connected segments corresponding to: Upper arm, lower arm, hand, and fingers. We assume that the first joint of the model connects the upper arm to a world coordinate frame. This model contains also simulated sensors on each segment. Based on the models movement simulated data can be acquired. The calibration goes on as follows:

1. Recording of calibration motion
2. Signal preprocessing (see section 4)
3. Apply measured orientations to the model (move the model)
4. Derive simulated data from model
5. Compare simulated data with measured data
6. Change parameters of the arm model to minimize the error. Continue with step 3.

Step 3 to 6 are repeated until the resulting error is small enough. So the calibration can be expressed as a optimization problem, where the distance between the measured data and the data derived from the model is minimized:

$$\min_{\vec{t}, \vec{q}, \vec{s}} \mathcal{D} [D_{\text{sensors}}, D_{\text{model}}(O_{\text{sensors}}, \vec{t}, \vec{q}, \vec{s})], \quad (3)$$

where:

- $\mathcal{D}$  is some distance function
- $D_{\text{sensors}}$  are data computed from the measured accelerations of the sensors
- $D_{\text{model}}$  are data computed with the arm model which depends on:
  - $O_{\text{sensors}}$  are measured orientation data
  - $\vec{t}$  position of each sensor on its corresponding segment
  - $\vec{q}$  orientation of each sensor with respect to its corresponding segment
  - $\vec{s}$  length of each segment

### 5.1 Optimization Problem

The optimization crucially depends on two different parameters. First the distance function  $\mathcal{D}$ . This function defines the similarity of two data sets  $D$ . As we have to compare data of different quality (i.e. position, orientation and length) different distance functions have to be considered. The actually used function  $\mathcal{D}$  may consist of one or any combination of different distance functions. The adequate combination

for our problem will be determined in the results. The three chosen basic distance functions are:

$$\mathcal{D}_E = \sqrt{(D_{\text{sensors}} - D_{\text{model}})^2} \quad (4)$$

$$\mathcal{D}_{\text{cos}} = \arccos \left( \left\langle \frac{D_{\text{sensors}}}{\|D_{\text{sensors}}\|}, \frac{D_{\text{model}}}{\|D_{\text{model}}\|} \right\rangle \right) \quad (5)$$

$$\mathcal{D}_{\text{dir}} = \|D_{\text{sensor}} - D_{\text{model}}\| \quad (6)$$

The second important parameter of the optimization problem is the kind of data  $D$  we use. For the optimization we only use measured acceleration data and quantities deduced from the acceleration. Hence the usable features are:

- $aG$ : local acceleration (measured data from sensors)
- $a$ : global acceleration (without gravitation)
- $v$ : velocity
- $p$ : position

Although all the deduced features are computed from the local acceleration, there is a difference in quality. As mentioned above the global acceleration is computed using the measured orientation. Therefore, methods like zero velocity updates are applicable. The velocity data  $v$  are obtained from integrating  $a$  and are smoother which could result in a more stable optimization. By additional integration we obtain position data  $p$ , which leads to a further generalization. So  $D$  may be any combination of those features.

The goal is to get  $D_{\text{sensors}}$ , the measured data, and  $D_{\text{model}}$ , the results from the model with respect to the chosen distance function as similar as possible. The movements of the model are produced by orientation data  $O_{\text{sensors}}$ . The arm model is configured by the segments length, position and the orientation of each sensor. Depending on this configuration the forward kinematics of the arm induced by  $O_{\text{sensors}}$  results in a specific movement. This movement generates the data  $D_{\text{model}}$ . This constitutes a non-linear optimization problem which we solved by using the Levenberg-Marquardt algorithm.

## 5.2 Calibration Motion

The result of the calibration step depends on the underlying movement. There is no need for specific given motion that has to be performed. However, the calibration motion should cover movements in any degree of freedom, if possible. As the calibration movement is used to determine the arm parameters, a wide range of different motions will result in a well defined solution. Also it is expected that the optimization process will converge faster. In general to

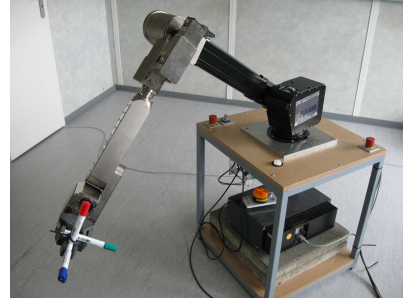


Figure 4: The used manipulator. Originally it is mounted on an EOD robot.

provide better results the calibration motion should include fast movements, pauses (for zero velocity updates) and movements in any possible direction. Note that the main part of the movements should be faster than the ZUPT threshold, otherwise the calibration might be unreliable. Experiments show that calibration movements of less than one minute are sufficient.

## 6 ROBOT ARM CONTROL

The manipulator used in our experiments is the robot arm normally mounted on the teleMAX robot of the manufacturer Telerob. The configuration is similar to a human arm, with two differences. First, it is equipped with a telescope joint. Second and more important, it is rotated by 90 degrees so that the shoulder does not turn vertically but horizontally (see Figure 4). The robot arm is equipped with a so called TCP control. With its help the tip of the gripper can be moved along and rotate around all axis. Every movement command is related to the point of origin in the shoulder joint. Using the inertial sensor based reconstruction of the human arm, the finger position can be determined and send to the manipulator. The goal of the presented control system is to give the operator a feeling for the movements of the manipulator. Therefore, the relation of human actions and robot reactions must be visible to the operator. If a movement is performed by the operator the manipulator has to react and imitate this movement. When designing the controller, one has to be kept in mind that the used manipulator is not able to perform movements as fast as humans.

To let the manipulator perform a similar trajectory as the operator, a list of end effector positions could be implemented. While the human performs the movement such a list is filled and the manipulator will move to the given end effector positions as fast as possible. We decided not to use such a technique

because of the speed gap between operator and manipulator. Experiments showed that in our setup there is no feeling of being directly coupled to the manipulator. The manipulator will be more and more behind the operator’s movements. Therefore, we decided to implement a direct transmission of the current operator’s arm position. This provides the operator with a feeling of being directly connected to the manipulator and, in contrast to the list, it is possible to interrupt a not desired movement. But to define a trajectory the TCP has to follow, the operator has to move in the same speed as the robot does. Otherwise only target points are given, which the robot tries to reach on a linear way.

Fully stretched the manipulator has a range of about 1.50 m, more than a human arm. To achieve the full length of the manipulator, there must be a scaling function between the human motion and the manipulator movement. In experiments with different users, seemed to scaling the up-down direction (the z-axis) provided an unnatural feeling. Scaling in x- and y-axis seemed to be no problem to adapt to. So a scaling for x- and y-axis is used to allow the operator to use the whole operation range of the manipulator. We decided not to use any scaling for the z-axis.

## 7 RESULTS

### 7.1 Calibration of Synthetic Examples

To test the calibration and the used optimizer, we first used synthetic data. The synthetic data were produced by the arm model. Here for, the model is moved and the simulated sensors provide us with acceleration and orientation data. As stated in Section 5 the calibration mechanism has to find the correct positioning of each of the four sensors and the length of the segment corresponding.

To check whether the optimizer can find the correct configuration we performed several experiments. On the one hand, we tested situations where only one of the parameters is erroneous. On the other hand we have configurations where all three parameters were unknown. For example we tested the calibration of the system with sensors erroneous in orientation. So the model was build up with the sensors in orientation not equal to the segment’s orientation. Movements were simulated and the sensor data computed. These sensor data were now used by the optimizer. It knows where the sensors are and how long each segment is. It does not know in which orientation the sensors are mounted. The experiment shows that the optimizer was able to determine the sensors’ orientations. The

	$D_c, D_{dir}$			$D_c, D_{cos}$			$D_{dir}, D_{cos}$			$D_c, D_{dir}, D_{cos}$		
	E(tr)	E(ori)	E(len)	E(tr)	E(ori)	E(len)	E(tr)	E(ori)	E(len)	E(tr)	E(ori)	E(len)
a, aG	0	0	0.01	0	0	0.02	0	0	0	0	0	0.01
a, v	0.29	0.12	0.11	0.11	0.08	0.07	0.25	0.07	0.07	0.23	0.09	0.08
aG, v	0.42	0	0.07	0.42	0	0.07	0.43	0	0.09	0.42	0	0.08
a, aG, v	0	0	0.02	0	0	0	0.01	0	0	0.41	0	0.05
a, aG, v, p	0	0	0.01	0.43	0	0.07	0.04	0	0.02	0	0	0.02

Figure 5: Some example results for calibration of synthetic data with all three parameters faulty. E(tr) is the error of the positioning of the sensors, E(ori) the error of the orientation, E(len) the error of the segment length.

described experiment was repeated with each parameter being erroneous and also with all three parameters erroneous.

As the optimizer itself is also parameterized, the output depends on the chosen combination of distance functions and the features chosen (see Section 5). To check which combination of distance functions and features is adequate to solve the problem, we tested every possible combination on the synthetic data. In figure 5 some results are given for the experiments with all three parameters erroneous.

There are some combinations which are not suitable to use but it shows that there are several different combinations of metrics and features which enable the optimizer to find the original arm configuration. This shows that the method is able to find the correct configuration in general. The next step is to see whether the system is also stable with real data.

### 7.2 Calibration of Real Sensor Data

To test how the calibration step is effective to the motion reconstruction on real data a ground truth is necessary. We used an optical motion capturing system to compare the real movement of the operator with the uncalibrated and calibrated reconstruction from our system. In Figure 6 two example movements are shown. The red crosses show the finger positions (used as target position for the TCP of the manipulator) of the uncalibrated system. The green circles show the calibrated reconstruction. The blue dots represent the data from the optical system. In the left picture a wiping motion is shown. The right digram shows a gripping motion. In both examples the calibrated system performs more precise with respect to the ground truth.

To show the effect of calibration to the motion reconstruction we used a poorly positioned system to reconstruct a stretched arm. In Figure 7 the wrong reconstruction can be seen. This flexed position happens due to the fact that the model expects the sensors to be aligned to the orientations of the segments. After the calibration step the model is very close to the real pose, but with a small error in the bended elbow.

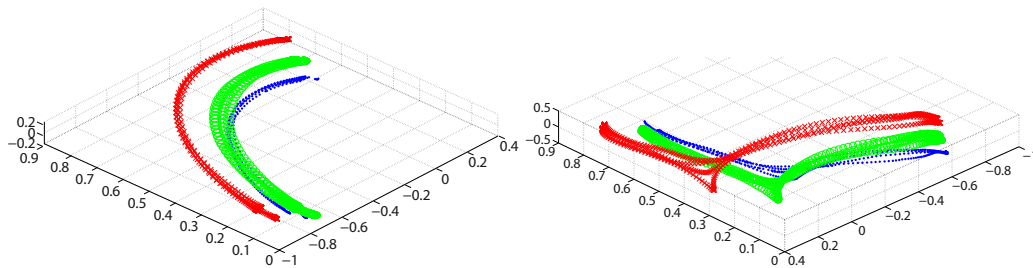


Figure 6: Comparison between an optical MoCap system as ground truth and our inertial sensor based system. The red crosses: finger positions of the uncalibrated system, green circles: calibrated reconstruction, blue dots: optical system.

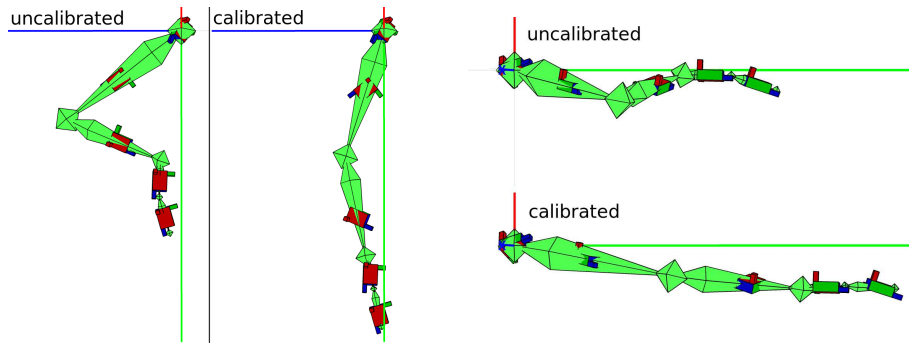


Figure 7: Arm model before and after calibration. The underlying pose is a stretched arm. As the sensors on upper and lower arm were not well orientated, the uncalibrated model returns a bended arm. After calibration the model shows are pose much more alike the operator’s actual arm configuration., a stretched arm. Left picture shows view from above, right picture from the side.

task	successful	failure	average time [s]
infinity	8	0	37
Pushing	8	0	49
Gripping	7	1	52

Table 1: Performance of untrained users with the control system.

task	successful	failure	average time [s]
infinity	14	0	34
Pushing	13	1	31
Gripping	12	2	35

Table 2: Performance of fairly trained users with the control system.

### 7.3 Control

To show that the presented method in general is adequate to control the manipulator we had different persons to perform several tasks. Those tasks were:

- Perform an infinity symbol
- Push a small log from the corner of a table
- Grip the log, (whereas the opening of the gripper is only slightly wider than the logs diameter)

Half of the users had never used this control method before. They had to perform each of the tasks twice. Once without any training, and once after some training. The results can be seen in Table 1 and 2.

Here you can see that, even totally untrained, most users were able to use the manipulator in the desired way. In fact the untrained test persons have a lower

failure rate as the trained people. This may result from the ambitions of the trained people to be faster. This seems to make them more careless.

Often expressed criticism was the gap between the speed of the manipulator and the human arm. Most users needed some time to adapt to the much slower manipulator. So we expect better results when using a more agile manipulator.

## 8 CONCLUSIONS

In this paper we presented a control method for a robot arm. The main requirements to fulfill were an intuitive control, simple usage, and little space consuming. Our system based on inertial sensors to be worn on the operator’s arm. With the help of an au-

tomatic calibration function, the exact placement of these sensors can be found, which makes an exact placement obsolete. Hence, equipping the system is rather simple and fast. The system is able to reconstruct the motion of the operator and therefore, send them to the manipulator. This results in a direct motion control where the user steers the TCP of the manipulator with his own movements. First experiments showed that even untrained persons can use the control system to fulfill certain tasks.

However, the system showed some points to improve, especially in its intuitive use. As it took a lot of time to get used to the fact, that the operator only steers the TCP but not the morphologies of the arm, a next step in development will be to map the reconstructed joint angles of the human arm to the joints of the manipulator to achieve a similar manipulator configuration compared to the operator's pose. Also a continuous calibration could be useful. The calibration as it is designed showed no reason not to be used parallel to the steering task. This enables the system to react to changes e.g. a loose sensor or changes in the magnetic field. Here experiments are necessary to show if the system stays stable.

## REFERENCES

- Bergamasco, M., Allotta, B., Bosio, L., Ferretti, L., Parrini, G., Prisco, G., Salsedo, F., and Sartini, G. (1994). An arm exoskeleton system for teleoperation and virtual environments applications. In *Robotics and Automation, 1994. Proceedings., 1994 IEEE International Conference on*, pages 1449–1454 vol.2.
- Chang, M. M. Y. (2006). Motion segmentation using inertial sensors. In *VRCIA '06: Proceedings of the 2006 ACM international conference on Virtual reality continuum and its applications*, pages 395–399, Hong Kong, China. ACM.
- Foxlin, E. (2005). Pedestrian tracking with shoe-mounted inertial sensors. *IEEE Comput. Graph. Appl.*, 25(6):38–46.
- Goertz, R. (1954). Mechanical master-slave manipulator. *Nucleonics*, 12(11):45–46.
- Grejner-Brzezinska, D. A., Yi, Y., and Toth, C. K. (2001). Bridging gps gaps in urban canyons: Benefits of zupt. *Navigation Journal*, 48(4):217–225.
- Laycock, S. and Day, A. (2003). Recent developments and applications of haptic devices. *Computer Graphics Forum*, 22(2):117–132(16).
- Lee, J. and Shin, S. Y. (2002). General construction of time-domain filters for orientation data. *IEEE Transactions on Visualization and Computer Graphics*, 8(2):119–128.
- Lee, J. C. (2008). Hacking the Nintendo Wii Remote. *IEEE Pervasive Computing*, 7(3):39–45.
- Miller, N., Jenkins, O. C., Kallmann, M., and Mataric, M. J. (2004). Motion capture from inertial sensing for untethered humanoid teleoperation. In *Proceedings of the IEEE-RAS International Conference on Humanoid Robotics (Humanoids)*, Santa Monica, CA.
- Pollard, N. S., Hodgins, J. K., Riley, M. J., and Atkeson, C. G. (2002). Adapting human motion for the control of a humanoid robot. In *Proceedings of International Conference on Robotics and Automation*, pages 1390–1397.
- Sabatini, A., Martelloni, C., Scapellato, S., and Cavallo (2005). Assessment of walking features from foot inertial sensing. *Biomedical Engineering, IEEE Transactions on*, 52(3):486–494.
- Schou, T. and Gardner, H. J. (2007). A wii remote, a game engine, five sensor bars and a virtual reality theatre. In *OZCHI '07: Proceedings of the 19th Australasian conference on Computer-Human Interaction*, pages 231–234, New York, NY, USA. ACM.
- Shiratori, T. and Hodgins, J. K. (2008). Accelerometer-based user interfaces for the control of a physically simulated character. In *SIGGRAPH Asia '08: ACM SIGGRAPH Asia 2008 papers*, number 5, pages 1–9, Singapore. ACM.
- Slyper, R. and Hodgins, J. K. (2008). Action capture with accelerometers. In *Proceedings of the 2008 ACM/Eurographics Symposium on Computer Animation*.
- Tachi, S., Arai, H., and Maeda, T. (1990). Tele-existence master-slave system for remote manipulation. In *Intelligent Robots and Systems '90. 'Towards a New Frontier of Applications', Proceedings. IROS '90. IEEE International Workshop on*, pages 343–348 vol.1.
- Tao, Y., Hu, H., and Zhou, H. (2007). Integration of vision and inertial sensors for 3D arm motion tracking in home-based rehabilitation. *The International Journal of Robotics Research*, 26(6):607–624.
- Vlasic, D., Adelsberger, R., Vannucci, G., Barnwell, J., Gross, M., Matusik, W., and Popović, J. (2007). Practical motion capture in everyday surroundings. In *SIGGRAPH '07: ACM SIGGRAPH 2007 papers*, page 35, New York, NY, USA. ACM Press.
- Welch, G. and Foxlin, E. (2002). Motion tracking: No silver bullet, but a respectable arsenal. *IEEE Comput. Graph. Appl.*, 22(6):24–38.
- Yokokohji, Y. and Yoshikawa, T. (1992). Bilateral control of master-slave manipulators for ideal kinesthetic coupling-formulation and experiment. In *Robotics and Automation, 1992. Proceedings., 1992 IEEE International Conference on*, pages 849–858 vol.1.
- Zhou, H. and Hu, H. (2007). Upper limb motion estimation from inertial measurements. *International Journal of Information Technology*, 13(1).
- Zhou, H., Hu, H., and Tao, Y. (2006). Inertial measurements of upper limb motion. *Medical and Biological Engineering and Computing*, 44(6):479–487.